

## Comparison of Adsorption of Nitrogen and Oxygen- Molecules on the Open Ended and Surface of Swcnts: A Computational NMR and NQR Study

F. Ashrafi, S.A. Babanegad and A.S. Ghasemi

Department of Chemistry, Payame Noor University, P.O. box 19395-3697, Tehran, Iran

**Abstract:** This study have performed for investigating on the results of adsorption of several gaseous molecules as nitrogen and oxygen, on the open-ended and external surface of H-capped (4, 4) armchair semiconducting Single-walled Carbon Nanotube (SWCNTs), using Density Functional Theory (DFT) calculations. Geometric optimizations were carried out at B3LYP/6-311G\*level of theory using Gaussian 98 program. Structural models are optimized and adsorption energies are obtained to investigate the nuclear magnetic resonance (NMR) and Nuclear Quadrupole Resonance (NQR) spectroscopy parameters for (nitrogen-CNTs) and (oxygen-CNTs) model of (4,4) armchair SWCNTs. The chemical-shielding ( $\sigma_{ii}$ ) tensors were converted to isotropic chemical-shielding ( $\sigma_{iso}$ ) and anisotropic chemical-shielding ( $\Delta\sigma$ ) and asymmetrical ( $\mu_i$ ) parameters of  $^{13}\text{C}$ ,  $^{15}\text{N}$  and  $^{17}\text{N}$  nucleus for the optimized structures. NMR calculations were evinced that  $^{13}\text{C}$  chemical shielding armchair (4,4) on the open ended and external surface is more sensitive to  $^{15}\text{N}$  and  $^{17}\text{O}$  molecules adsorption compared to armchair (4,4) nanotubes. However, NMR parameters vary with the tube diameter. Chemical shielding tensors of  $^{15}\text{N}$  and  $^{17}\text{O}$  on the surface increase to chemical shifts open ended in the physisorption and increase in the open ended to the surface of SWCNTs armchair (4, 4). DFT calculations were performed to calculate  $^{14}\text{N}$  and  $^{17}\text{O}$  NQR spectroscopy parameters in the representative considered model of (4, 4) armchair SWCNTs.

**Key words:** DFT, isotropic chemical-shielding, NMR, NQR, physisorption, single-walled carbon nanotube

### INTRODUCTION

Carbon nanotubes, discovered by Ijima (1993), are members of the fullerene family (Ijima *et al.*, 1993). The study of the gas adsorption on SWCNTs is nowadays the centre of interesting theoretical studies (Jang *et al.*, 2004; Valentini *et al.*, 2004; Wang *et al.*, 2004). Considering that the gas adsorption on SWCNTs modifies sensibly of their electronic properties, (Kong *et al.*, 2000), have proposed the use of SWCNTs as gas sensors. The adsorption behavior of gas molecules on the open ended and external surface of SWCNTs has been studied extensively in the past decade by theoretical calculation (Peng and Cho, 2000; Babanejad *et al.*, 2010; Ashrafi *et al.*, 2010; Ghasemi *et al.*, 2010; Lu *et al.*, 2005; Liu *et al.*, 2006; Ding *et al.*, 2004; Zhao *et al.*, 2005). Peng and Cho (2000) reported the calculation results of to nitrogen and oxygen molecules attached on the open-ended and external surface of SWCNTs by Density Functional Theory (DFT) based on B3LYP/6-311G\*level and GIAO method and found that the interaction between nitrogen and oxygen molecules and SWCNTs caused vigorous changes in the electrical resistivity of SWCNTs and thus could be used to detect gas molecules (Lu *et al.*, 2005). Because the derived well defined one dimensional

structure of SWCNTs has distinctive properties in mechanical, chemical and electronic aspects (Ijima *et al.*, 1993). The calculation of NMR parameters using DFT techniques have become a major and powerful tool in investigation of molecular structure (Duer, 2001).

Chemical shielding ( $\sigma_{ii}$ ) tensors originating the sites of these nuclei are measured trusty, produced by high-level quantum chemical calculations (Mirzaei and Hadipour, 2006; Wu *et al.*, 2002). Band structure calculations, using different quantum mechanical and semi-empirical methods have predicted electronic transport properties of SWCNTs (Mintmire *et al.*, 1992; Hamada *et al.*, 1992; Blase *et al.*, 1994; Charlier and Lambin, 1998). Interactions between nitrogen and oxygen molecules and SWCNTs have been signified in modifying the intrinsic SWCNTs electronic band gap (Charlier and Lambin, 1998). The tip gate changes the potential of localized defect states, so that the defect energy levels move in and out of resonance with the nanotube Fermi level. There is a considerable anisotropy in structure of graphite. Such anisotropy in properties, particularly in electrical properties, can be wholly advantageous. In connection with the size of the nanotubes, it is useful mentioning at this stage that as will be seen from the studiesb verified in later sections, many computational

studies involving standard nanotubes have focused on the use of (4, 4) nanotube, having a diameter of 5.67Å.

Nanotubes can be semiconductors depending on their diameter and twist, they display highly interesting features. In this topic, we provide first principles calculations on individual SWCNTs with adsorption of variety of gas molecules including nitrogen and oxygen molecules. Thus, <sup>15</sup>N and <sup>17</sup>O were applied for NMR of armchair (4, 4) SWCNTs and are studied by DFT method.

NQR measures the nuclear quadrupole coupling constant C<sub>Q</sub> which is the interaction energy of nuclear electric quadrupole moment eQ with the electric field gradient (EFG) tensors at the site of nucleus (Bailey *et al.*, 2000). Nuclei with a nuclear spin angular momentum greater than one-half (I>1/2) are so called quadrupoles. <sup>14</sup>N and <sup>17</sup>O have active nuclei in NQR spectroscopy measurements. The EFG tensors are very sensitive elements to the electrostatic environments at the sites of quadrupole nuclei, and can reveal new trends about electrostatic environment of SWCNTs (Mirzaei and Hadipour, 2006; Mirzaei and Hadipour, 2007). Computationally, the EFG tensors are calculated where they are proportional to C<sub>Q</sub>, therefore, quantum chemical calculations of the EFG tensors allow appraisal of measurable NQR parameters, and compare with the results of NMR.

### COMPUTATIONAL METHODOLOGY

The first principles calculations based on the DFT were performed in this investigation with the Generalized Gradient Approximation (GGA) by (Perdew *et al.*, 1996). In the present study, we investigate the effects of oxygen and nitrogen molecules chemisorption and physisorption on surface and open ended SWCNTs of armchair (4, 4). In order to investigate the electronic structure at the semiconductor SWCNTs contacts of oxygen and nitrogen molecular, the computations were fully executed by Gaussian 98 Software package (Frisch *et al.*, 1998; Barros *et al.*, 2007; Souza Filho *et al.*, 2007; Souza Filho *et al.*, 2006). Geometric optimizations were performed using 6-311G\* basis set with DFT/B3LYP functional (Parr and Yang, 1994; Becke, 1993).

NMR <sup>17</sup>O, <sup>15</sup>N and <sup>13</sup>C chemical shielding calculations were computed at B3LYP/6-311G\* level of theory using Gauge Including Atomic Orbitals (GIAO) approach (Wolinski *et al.*, 1990). The modeled armchair (4,4) consisted of 40 C atom with length of 4.8 Å was chosen for the purpose. In absence of periodic boundary conditions in molecular calculations, it is necessary to saturate the carbon dangling bonds with hydrogen atoms. Curvature of small tubes is a crucial characteristic responsible for intense interaction of atoms in tubes. Quantum chemical calculated tensors at the Principal Axes System (PAS) (σ<sub>11</sub> ≤ σ<sub>22</sub> ≤ σ<sub>33</sub>) is converted to a diagonal matrix with σ<sub>11</sub>, σ<sub>22</sub> and σ<sub>33</sub> components, measurable NMR parameters, chemical shielding

isotropic (σ<sub>iso</sub>) and chemical shielding anisotropic (Δσ) and asymmetrical (μ<sub>j</sub>) using, respectively (Duer, 2001).

This shows a second order change in molecular energy, as was indicated in following equation:

$$E = E_0 + B_0 \chi B_0 + \sum_{i=1}^N \mu_i \sigma B_0 + \dots \quad (1)$$

The summation is taken over the N nucleus in the system. We are not interested in the magnetic susceptibility, C<sub>Q</sub>, but only in the bilinear response property, thus we have following equation:

$$\sigma_{ij} = \left( \frac{\partial^2 E}{\partial B_i \partial \mu_j} \right) B_i = \mu_j \rightarrow 0 \quad (2)$$

where μ<sub>j</sub> and B<sub>i</sub> is the components of magnetic moment and external magnetic field, respectively.

The principal components for specification of shielding are defined by this coordinate system as following equations (Marian and Gastreich, 2001):

$$\sigma_{iso} = \frac{\sigma_{11} + \sigma_{22} + \sigma_{33}}{3} \quad (3)$$

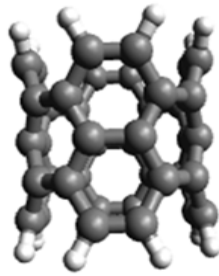
$$\Delta \sigma = \frac{3}{2} (\sigma_{33} - \sigma_{iso}) \quad (4)$$

$$\eta_\sigma = \frac{3}{2} \left( \frac{\sigma_{22} - \sigma_{11}}{\Delta \sigma} \right) \quad (5)$$

where σ<sub>iso</sub>, Δσ and μ<sub>j</sub> are isotropic, anisotropic and asymmetric parts of tensor, respectively and in certain cases vanishes. Quantum chemical calculations computational measurable NQR parameters, nuclear quadrupole coupling constant C<sub>Q</sub>, and asymmetry parameter η<sub>Q</sub>, and the calculated EFG tensors computational measurable parameters C<sub>Q</sub>, is the interaction energy of the nuclear electric quadrupole moment eQ and the EFG tensors, whereas η<sub>Q</sub> is a measure of the EFG tensors, deviation from cylindrical symmetry at the sites of quadrupole nucleus. Geometric optimizations and EFG calculations were performed using 6-311G\* basis set with B3LYP functional (Kang, 2006; Hou *et al.*, 2004). The interaction between nuclear electric quadrupole moment and EFG at quadrupole nucleus is described with following Hamiltonian (Abragam, 1961),

$$\hat{H} = \frac{e^2 q_{zz} Q}{4I(2I-1)} \left\{ 3\hat{I}_z^2 - I(I+1) + \frac{\hat{1}}{2} \eta Q (\hat{I}_x^2 - \hat{I}_y^2) \right\} \quad (6)$$

where q<sub>zz</sub> is the largest component of the EFG tensor in the principal axes frame, ηQ = |(q<sub>yy</sub> - q<sub>ss</sub>)/q<sub>ss</sub>|, and 0 ≤ ηQ ≤ 1, eQ, is the quadrupole moment of the nucleus and

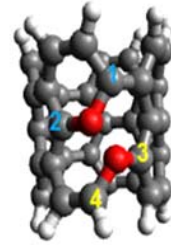


CNT (4,4)

Fig. 1: Carbon nanotube armchair (4, 4) model



CNT(4,4)-O<sub>2</sub>(A<sub>1</sub>)

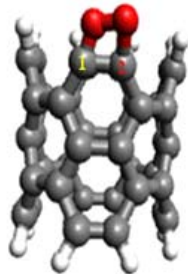


CNT(4,4)-O<sub>2</sub>(A<sub>2</sub>)

Fig. 4: Oxygen molecules chemisorption and physisorption on external surface of SWCNTs of armchair (4, 4)

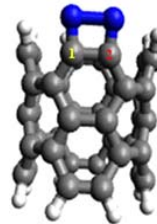


CNT (4,4)-O<sub>2</sub> D<sub>1</sub>

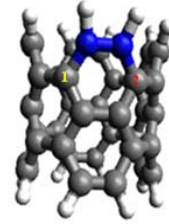


CNT (4,4)-O<sub>2</sub> D<sub>2</sub>

Fig. 2: Oxygen molecules chemisorption and physisorption on open ended of SWCNTs of armchair (4, 4)

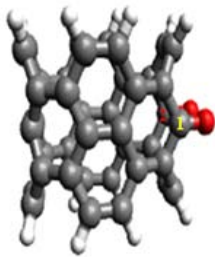


CNT (4,4)-N<sub>2</sub> D<sub>1</sub>

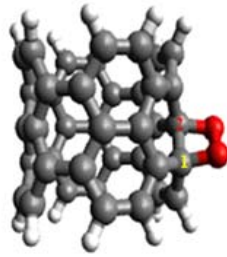


CNT (4,4)-N<sub>2</sub> D<sub>2</sub>

Fig. 5: Nitrogen molecules chemisorption and Physisorption on open ended of SWCNTs of armchair (4, 4)

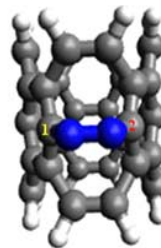


CNT (4,4)-O<sub>2</sub> A<sub>1</sub>

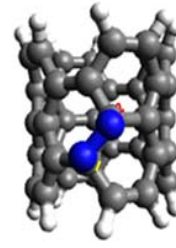


CNT (4,4)-O<sub>2</sub> A<sub>2</sub>

Fig. 3: Oxygen molecules chemisorption and physisorption on external surface of SWCNTs of armchair (4, 4)

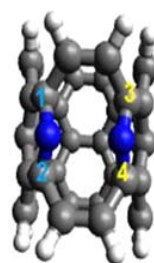


CNT (4,4)-N<sub>2</sub> A<sub>1</sub>

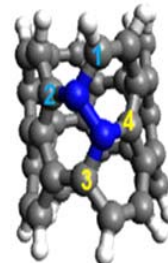


CNT (4,4)-N<sub>2</sub> A<sub>2</sub>

Fig. 6: Nitrogen molecules chemisorption and physisorption on external surface of SWCNTs of armchair (4, 4)



CNT(4,4)-N<sub>2</sub>(A<sub>1</sub>)



CNT(4,4)-N<sub>2</sub>(A<sub>2</sub>)

Fig. 7: Nitrogen molecules chemisorption and physisorption on external surface of SWCNTs of armchair (4, 4)

I is the spin of the nucleus. The principal components of the EFG tensor,  $q_{ii}$ , are computed in atomic unit  $1 \text{ au} = 9.717365 \times 10^{21} \text{ V/m}^2$ , with  $|q_{xx}| \leq |q_{yy}| \leq |q_{zz}|$  and  $q_{xx} + q_{yy} + q_{zz} = 0$ .

As a spin 1 nucleus with  $\eta \neq 0$  the  $^{15}\text{N}$  and  $^{17}\text{O}$  nucleus that measures the deviation of EFG tensor from axial symmetry (Marian and Gastreich, 2001). The computed  $q_{zz}$  component of EFG tensor is used to obtain nuclear quadrupole coupling constant from the equation (Lucken, 1969).  $C_Q(\text{MHZ})e^2q_{zz}Q^h$

Table 1: Comparison of chemical shielding and chemical shift tensors physisorption on the surface and open ended <sup>15</sup>N, <sup>17</sup>O NMR parameters for CNTs, Nitrogen-CNTs (4, 4) and Oxygen-CNTs (4, 4) systems<sup>a</sup>

Model	<sup>15</sup> N, <sup>17</sup> O	Atom	$\sigma_{ii} (\sigma_{11}, \sigma_{22}, \sigma_{33})^b$	$\sigma_{iso}$	$\Delta\sigma$	$\eta_\sigma$
CNT4,4-O <sub>2</sub> D <sub>1</sub>	O <sub>1</sub>	C <sub>1</sub>	(-94.7701; 0.8185; 83.1939)	-3.5859	130.1683	1.1015
	O <sub>2</sub>	C <sub>2</sub>	(-94.7683; 0.8351; 83.1889)	-3.5814	119.4113	1.2009
NT4,4-N <sub>2</sub> D <sub>2</sub>	N <sub>1</sub>	C <sub>1</sub>	(-128.6994; 28.0706; 83.1526)	-5.8312	133.4757	1.7620
	N <sub>2</sub>	C <sub>2</sub>	(-128.6994; 28.2120; 83.0000)	-5.8291	133.2437	1.7664
CNT4,4-O <sub>2</sub> A	O <sub>1</sub>	C <sub>1</sub>	(-80.4572; 10.7847; 102.7393)	11.0223	137.5755	0.9948
	O <sub>2</sub>	C <sub>2</sub>	(-80.8301; 10.9026; 102.4569)	10.8431	137.4207	1.0013
CNT4,4-O <sub>2</sub> A <sub>2</sub>	O <sub>1</sub>	C <sub>1</sub>	(40.2230; 40.2230; 141.8900)	96.4600	68.1450	0.0000
	O <sub>2</sub>	C <sub>2</sub>	(64.9425; 91.1836; 133.1339)	96.4200	55.0709	0.7147
CNT4,4-N <sub>2</sub> A <sub>1</sub>	N <sub>1</sub>	C <sub>1</sub>	(-88.7059; 38.8741; 95.3872)	15.1851	120.3032	1.5907
	N <sub>2</sub>	C <sub>2</sub>	(-88.7419; 38.8274; 95.3910)	15.1588	120.3483	1.5900
CNT4,4-N <sub>2</sub> A <sub>2</sub>	N <sub>1</sub>	C <sub>1</sub>	(85.6400; 85.6400; 120.5500)	97.2764	34.9100	0.0000
	N <sub>2</sub>	C <sub>2</sub>	(86.0700; 86.0700; 125.8100)	99.3120	39.7400	0.0000

<sup>a</sup>: Calculated  $\sigma_{ii}$ ,  $\sigma_{iso}$ ,  $\Delta\sigma$  values in ppm; <sup>b</sup>: In each row, the first number is for  $\sigma_{11}$ , the second number is for  $\sigma_{22}$ , and the third number is for  $\sigma_{33}$

Table 2: Comparison of chemical shielding and chemical shift tensors chemisorption on the surface and open ended <sup>15</sup>N, <sup>17</sup>O NMR parameters for CNTs, Nitrogen-CNTs and Oxygen-CNTs armchair(4, 4) systems<sup>a</sup>

Model	<sup>15</sup> N, <sup>17</sup> O	Atom	$\sigma_{ii} (\sigma_{11}, \sigma_{22}, \sigma_{33})^b$	$\sigma_{iso}$	$\Delta\sigma$	$\eta_\sigma$
CNT(4,4)-N <sub>2</sub> (D <sub>1</sub> )	N <sub>1</sub>	C <sub>1</sub>	(85.6400; 85.6400; 120.5500)	47.2827	176.1143	0.1897
	N <sub>2</sub>	C <sub>2</sub>	(86.0700; 86.0700; 125.8100)	46.5658	182.5256	0.1729
CNT(4,4)-O <sub>2</sub> (D <sub>2</sub> )	O <sub>1</sub>	C <sub>1</sub>	(-8.9800; -8.9800; 103.1800)	28.4067	98.6900	0.0000
	O <sub>2</sub>	C <sub>2</sub>	(-8.9700; -8.9700; 103.2000)	28.4200	112.1700	0.0000
CNT(4,4)-N <sub>2</sub> (A <sub>1</sub> )	N <sub>1</sub>	C <sub>1</sub>	(-65.7148; 14.9561; 129.4085)	26.2166	154.7878	4.6156
	N <sub>2</sub>	C <sub>2</sub>	(-65.6491; 14.9320; 129.3856)	26.2228	154.7442	4.6094
		C <sub>4</sub>	(-65.6564; 14.9540; 29.4354)	26.2443	66154.7472	4.6073
CNT(4,4)-N <sub>2</sub> (A <sub>2</sub> )	N <sub>1</sub>	C <sub>1</sub>	(-34.9738; 44.0376; 17.5517)	42.2052	113.0197	2.8081
		C <sub>2</sub>	(-76.9772; -39.0220; 120.5170)	1.5059	178.51	37.8064
	N <sub>2</sub>	C <sub>3</sub>	(-76.2848; -20.9271; 30.6033)	11.1305	179.2092	7.4603
		C <sub>4</sub>	(-55.4982; 63.6156; 121.5112)	43.2095	117.4526	4.1350
CNT(4,4)-O <sub>2</sub> (A <sub>1</sub> )	O <sub>1</sub>	C <sub>1</sub>	(-66.8441; 54.0845; 83.9711)	23.7372	90.3508	2.0077
		C <sub>2</sub>	(-66.4764; 53.8616; 84.4001)	23.9229	90.7075	1.9900
	O <sub>2</sub>	C <sub>3</sub>	(-66.7714; 54.0846; 83.9711)	23.7491	90.3313	2.0063
		C <sub>4</sub>	(-66.3669; 54.0373; 84.4001)	23.9226	90.262	2.0009
CNT(4,4)-O <sub>2</sub> (A <sub>2</sub> )	O <sub>1</sub>	C <sub>1</sub>	(-53.8794; 39.8243; 95.9593)	27.3014	102.9869	1.3648
		C <sub>2</sub>	(-43.5238; 12.7128; 100.4479)	1.5456	118.3535	0.7761
	O <sub>2</sub>	C <sub>3</sub>	(-29.8179; 7.3599; 103.6236)	27.0552	114.8526	0.4856
		C <sub>4</sub>	(-66.1822; 56.8643; 97.6708)	29.4509	102.3298	1.8037

<sup>a</sup>: Calculated  $\sigma_{ii}$ ,  $\sigma_{iso}$ ,  $\Delta\sigma$  values in ppm; <sup>b</sup>: In each row, the first number is for  $\sigma_{11}$ , the second number is for  $\sigma_{22}$ , and the third number is for  $\sigma_{33}$

Table 3: Calculated <sup>13</sup>C EFG parameters in Nitrogen-CNTs (4, 4) and Oxygen-CNTs (4, 4) for surface and open ended systems<sup>a</sup>

Model	Atom	$q_{xx}$	$q_{yy}$	$q_z$	$\eta_\sigma$	$C_o$
CNT(4,4)-O <sub>2</sub> (D <sub>1</sub> )	C <sub>1</sub>	0.036258	0.176217	-0.212475	0.66	-1.2778
	C <sub>2</sub>	0.068046	0.175906	-0.243952	0.44	-1.4672
CNT(4,4)-O <sub>2</sub> (D <sub>2</sub> )	C <sub>1</sub>	0.105828	0.135165	-0.240993	0.12	-1.4494
	C <sub>2</sub>	0.147502	0.163109	-0.310611	0.05	-1.8680
CNT(4,4)-N <sub>2</sub> (D <sub>1</sub> )	C <sub>1</sub>	0.108751	0.217084	-0.325835	0.33	-1.5659
	C <sub>2</sub>	0.108786	0.216949	-0.325735	0.33	-1.5654
CNT(4,4)-N <sub>2</sub> (D <sub>2</sub> )	C <sub>1</sub>	-0.064501	-0.185988	0.250489	0.48	1.2038
	C <sub>2</sub>	-0.064547	-0.185807	0.250354	0.48	1.2031
CNT(4,4)-O <sub>2</sub> (A <sub>1</sub> )	C <sub>1</sub>	0.114913	0.217092	-0.332005	-0.33	-1.9967
	C <sub>2</sub>	0.115191	0.217377	-0.332568	0.30	-2.0001
CNT(4,4)-O <sub>2</sub> (A <sub>2</sub> )	C <sub>1</sub>	0.056708	0.235503	0.235503	0.61	-1.7574
	C <sub>2</sub>	0.134179	0.172331	-0.306510	0.12	-1.8434
CNT(4,4)-N <sub>2</sub> (A <sub>1</sub> )	C <sub>1</sub>	0.062574	0.133920	-0.196494	0.36	-0.9443
	C <sub>2</sub>	0.007669	0.136100	-0.143769	0.89	-0.6909
CNT(4,4)-N <sub>2</sub> (A <sub>2</sub> )	C <sub>1</sub>	0.046359	0.090398	-0.136757	0.32	-0.6572
	C <sub>2</sub>	0.037639	0.158783	-0.196422	0.62	-0.9439

<sup>a</sup>: All  $q_{ii}$  values in atomic units (1au = 9.717365 10<sup>21</sup>/Vm<sup>2</sup>)

## RESULTS and DISCUSSION

In present study, two models of armchair (4, 4) SWCNTs with specified tube lengths are studied using

quantum chemical calculations (Fig. 1 to 7). Chemical shielding and EFG tensors model of (4, 4) SWCNTs interacted with oxygen and nitrogen molecules were obtained. The calculated geometric parameters <sup>15</sup>N, <sup>17</sup>O

and  $^{13}\text{C}$  chemical shielding and EFG tensors are presented in Table (1-3). In the following sections, molecular geometries and NMR chemical shielding and NQR tensors resulted from  $^{17}\text{O}$  and  $^{15}\text{N}$  molecular chemisorptions and physisorption are discussed, separately.

**The chemisorption and physisorption  $^{17}\text{O}$  and  $^{15}\text{N}$  NMR parameter modeled of armchair (4, 4) the surface and open end:** Table 1 and 2 exhibits the calculated  $^{13}\text{C}$  chemical shielding tensors for SWCNTs. Nitrogen and Oxygen molecules chemisorption and physisorption on external surface and open ended of CNTs has a significant influence on  $^{13}\text{C}$  NMR tensors, which is in complete accordance with the facts mentioned above previously. Consequently, it has been  $^{17}\text{O}$  and  $^{15}\text{N}$  indicated that for the H-capped SWCNTs, the calculated  $^{13}\text{C}$  chemical shielding values physisorption are smaller at the open ended of tube, compared to the surface, if the carbon is directly bound to hydrogen, unless, it is larger (Liu *et al.*, 2007). To assess the dependence of NMR results on carbon atom position,  $^{13}\text{C}$  chemical shielding isotropy values of armchair (4, 4) CNTs have calculated on surface and open ended  $^{15}\text{N}$  and  $^{17}\text{O}$  of  $^{13}\text{C}$  adsorption (Table 3). Two different parts of surface tube axis and open ended are considered. Interesting open end is evidenced: for armchair (4, 4) CNTs, the isotropy physisorption  $^{17}\text{O}$  and  $^{15}\text{N}$  of  $^{13}\text{C}$  shielding tensor are larger at the surface compared to the open end. It is also show that the chemical shielding components converge in a way similar to that of the chemical shifts when increasing the tube length even though not as smoothly as the isotropic shielding. Chemical shielding tensors and chemical shifts are efficient parameters for characterization of single walled carbon nano tubes. Calculation of these shielding tensors for oxygen and nitrogen nuclei reveals that increasing length and diameter of CNTs (4, 4) chemical shielding will cause oxygen and nitrogen nuclei converge on the single walled nano tube surface and open ended; the results are consistent with strong interaction physisorption between the tube and oxygen molecules in CNT(4,4)- $\text{N}_2(\text{A}_2)$ . This is consistent with previous results derived from band structure calculations (Rubio *et al.*, 1994; Balase *et al.*, 1994). On the other hand, the calculated  $^{17}\text{O}$  and  $^{15}\text{N}$  chemical shielding values in the middle of the open ended CNT (4,4) and surface seem close to the values -3.58 ppm, -5.83 ppm and 10.84 ppm, 96.46 ppm, respectively (Table 1). The calculated  $^{17}\text{O}$  and  $^{15}\text{N}$  chemical shielding of the surface CNTs armchair(4,4) and open ended seem close to the values 53.8495, 54.1090, 78.5398 and 149.1663 ppm, respectively (Table 2). More recently, it is indicated that introduction of oxygen atoms is theoretically predicted to give rise to chiral current flow along the nanotube (Zurek *et al.*, 2008) due to symmetry breaking (Liu and Guo, 2004; Miyamoto, 1996). The results deduced from comparison of sites ( $\text{A}_1$ ,  $\text{A}_2$ ,  $\text{D}_1$  and

$\text{D}_2$ ), show that the carbon atoms included in oxygen and nitrogen molecular chemisorption and physisorption become more shielded. Among the six NMR principal components, intermediate shielding component,  $\sigma_{22}$ , shows more change from SWCNTs compared with surface and open ended the oxygen-CNTs and nitrogen-CNTs system. The interest of oxygen and nitrogen CNTs in terms of application is the control of the type of charge carriers within the CNTs. Oxygen-CNTs and nitrogen-CNTs should show significant advantages over CNTs for gas sensor applications, due to their reactive tube surfaces and open ended and the sensitivity of their transport characteristics in relation with the presence, distribution and chemistry of oxygen. Peng and Cho (2003) first suggested oxygen-CNTs and nitrogen- CNTs for use in gas sensors, due to the ability of doped molecular oxygen and nitrogen to bind to incoming gas species. The molecular oxygen and nitrogen in the CNTs can be seen as regular defects which change the chemical and physical behavior of the CNTs.

**The chemisorption and physisorption  $^{17}\text{O}$  and  $^{14}\text{N}$  NQR parameter of armchair (4, 4) model on the surface and open end:** The calculated NQR parameters at the sites of  $^{14}\text{N}$  and  $^{17}\text{O}$  nuclei are shown in Table 3 for armchair (4, 4) models of oxygen-CNTs and nitrogen-CNTs. The quadrupole moment is nonzero only for nucleuses with spin quantum number,  $I$ , greater than or equal to 1. This is a nuclear physics and chemistry parameter describing the distribution of charge in the nucleus. In CNT (4, 4)-  $\text{O}_2(\text{D}_1)$ , coupling to the EFG of the valence electrons is largely based on chemistry, although the local crystal packing also plays a role. The  $q_{yy}$  values of those nucleuses which participate in the intermolecular H-bonding interactions decrease, but their  $\eta_Q$  values increase for chemisorption of molecular nitrogen and oxygen on open ended regarding to their physisorption on open ended. The magnitude of these changes for each nucleus depends on its contribution to the interactions. Therefore, more changes in each nucleus NQR parameter indicate its greater role among the other nucleuses in contributing to CNTs. The calculated parameter with the 6-311G\* basis sets is in good consistent. In this section, the calculated  $^{14}\text{N}$  and  $^{17}\text{O}$  quadrupole coupling tensors,  $q_{ii}$ , quadrupole coupling constant,  $C_Q$ , and asymmetry parameter,  $\eta_Q$ , of the  $^{14}\text{N}$  and  $^{17}\text{O}$  molecular in surface and open ended of SWCNTs is discussed. As shown in (Fig. 1) Due to this contribution to CNTs interaction,  $^{14}\text{N}$  quadrupole coupling tensors for the target molecule in the CNTs deviate considerably from  $^{17}\text{O}$  values. As shown in Table 3, both  $q_{xx}$  and  $q_{yy}$  tensor components increase from  $^{17}\text{O}$  to  $^{14}\text{N}$ , whereas  $q_{xx}$  or  $C_Q$  expose opposite tendency. This is also reflected in the calculated asymmetry parameter. As a general trend, from the monomer to the target molecule in the cluster, H-bonding interactions reduce the calculated  $^{14}\text{N}$  and  $^{17}\text{O}$

quadrupole coupling constant values whereas increase the asymmetry parameter.

This tensor becomes almost asymmetric for the target molecule in the CNTs cluster. The  $\eta_Q$  values for molecular nitrogen and oxygen change is 0.89MHz-0.05 MHz and CQ values for molecular nitrogen and oxygen change is 1.2038-2.0001 MHz units from the monomer to the target molecule in the cluster, respectively.

While EFG tensor at  $^{14}\text{N}$  and  $^{17}\text{O}$  sites is approximately axially symmetric,  $\eta_Q \approx 0$ , from the gas-phase isolated molecule to the monomer molecule in solid phase.

### CONCLUSION

We have presented a systematic computational study on molecular oxygen and nitrogen interactions of SWCNTs structure. Conformation and a quantum-chemical calculation by the GIAO calculations at the B3LYP/6-311G\* level using DFT optimized geometries provided isotropic shielding tensors that correlated well with the observed chemical shift data. The calculated NMR tensors at the sites of  $^{15}\text{N}$  and  $^{17}\text{O}$  nucleus and EFG tensors of  $^{14}\text{N}$  and  $^{17}\text{O}$  nucleus, in armchair CNTs (4, 4) model, put on evidence that isotropy of physisorption  $^{17}\text{O}$  and  $^{15}\text{N}$  of  $^{13}\text{C}$  shielding tensor are larger at the surface compared to the open end. Calculation of chemical shielding tensors and chemical shifts for oxygen and nitrogen nucleus reveals that increasing length and diameter of CNTs (4, 4) chemical shielding will cause oxygen and nitrogen nucleus converge on the single walled nanotube surface and open ended. The results are consistent with strong interaction physisorption between the tube and oxygen molecules in CNT (4, 4)- $\text{N}_2(\text{A}_2)$ . The results also show that the chemical shielding tensors and chemical shifts are efficient parameters for characterization of single walled carbon nanotubes. While the NMR and EFG tensors at the sites of various nuclei are not similarly influenced by these interactions. More changes in each nucleus NQR parameter indicate its greater role among the other nuclei in contributing to CNTs. Among other nuclei of SWCNTs, molecular oxygen and nitrogen are those nuclei which their NMR and EFG tensors are considerably influenced by CNTs interactions.

### REFERENCES

Abraham, A., 1961. Principles of Nuclear Magnetism. Clarendon Press, Oxford, pp: 599, OCLC Number: 242700.  
Ashrafi, F., A.S. Ghasemi, S.A. Babanejad and M. Rahimova, 2010. Optimization of carbon nanotubes for nitrogen gas adsorption. Res. J. Appl. Sci. Eng. Tech., 2(6): 547-551.

Babanejad, S.A., F. Ashrafi and A.S. Ghasemi, 2010. Optimization of adsorption of oxygen gas on Carbon nanotubes surface. Archives Appl. Sci. Res., 2(5): 438-443.  
Bailey, W.C., D.F.T. Chem and HF-DFT, 2000. Calculations of  $^{14}\text{N}$  quadrupole coupling constants in Molecules. Phys., 252; 57-66.  
Balase, X., A. Rubio, S.G. Louie and M.L. 1994. Cohen, stability and band gap constancy of boron-nitride Nanotubes. Europhys. Let., 28: 335.  
Blase, X., L. Benedict, E.L. Shirley and S.G. Louie, 1994. Are fullerene tubules metallic? Phys. Rev. B, 57: 1878.  
Barros, E.B., H. Son, G.G. Samsonidze, A.G. Souza Filho, R. Saito, Y.A. Kim, H. Muramatsu, T. Hayashi, M. Endo, J. Kong and M.S. Dresselhaus, 2007. Raman spectroscopy of double-walled carbon nanotubes treated with  $\text{H}_2\text{SO}_4$ . Phys. Rev. B, 76(4): 045425.  
Becke, A.D., 1993. Density-functional thermochemistry. III: The role of exact exchange. J. Chem. Phys., 98: 5648.  
Charlier, J.C. and P. Lambin, 1998. Electronic structure of carbon nanotubes with chiral symmetry. Phys. Rev. B, 57(24): R15037.  
Ding, F., K. Bolton and A. Rosen, 2004. Nucleation and growth of single-walled carbon nanotubes: A molecular dynamics study. J. Phys. Chem. B, 108: 17369.  
Duer, M.J., 2001. Solid State NMR Spectroscopy: Principles and Applications. Blackwell Science Ltd., London, ISBN: 9780632053513.  
Frisch, M.J., G.W. Trucks, H.B. Schlegel, G.E. Scuseria, M.A. Robb, J.R. Cheese-man, V.G. Zakrzewski, J.A. Montgomery Jr., R.E. Stratmann, J.C. Burant, S. Dapprich, J.M. Millam, A.D. Daniels, K.N. Kudin, M.C. Strain, O. Farkas, J. Tomasi, V. Barone, M. Cossi, R. Cammi, B. Mennucci, C. Pomelli, C. Adamo, S. Clifford, J. Ochterski, G.A. Petersson, P.Y. Ayala, Q. Cui, K. Morokuma, D.K. Malick, A.D. Rabuck, K. Raghavachari, J.B. Foresman, J. Cioslowski, J.V. Ortiz, A.G. Baboul, B.B. Stefanov, G. Liu, A. Liashenko, P. Piskorz, I. Komaromi, R. Gomperts, R.L. Martin, D.J. Fox, T. Keith, M.A. Al-Laham, C.Y. Peng, A. Nanayakkara, C. Gonzalez, M. Challacombe, P.M.W. Gill, B. Johnson, W. Chen, M.W. Wong, J.L. Andres, C. Gonzalez, M. Head-Gordon, E.S. Replogle and J.A. Pople, 1998. Gaussian 98. Gaussian Inc., Pittsburgh PA.  
Ghasemi, A.S., F. Ashrafi, S.A. Babanejad and M. Rahimova, 2010. A computational NMR study of chemisorption of nitrogen-doped on the surface of single-walled carbon nanotubes. Arch. Appl. Sci. Res., 2(4): 262.

- Hamada, N., S. Sawada and A. Oshiyama, 1992. New one-dimensional conductors: Graphitic microtubules. *Phys. Rev. Let.*, 68: 1579.
- Hou, S., Z. Shen, J. Zhang, X. Zhao and Z. Xue, 2004. Ab initio calculations on the open end of single-walled BN nanotubes. *Chem. Phys. Let.*, 393(1-3): 179.
- Ijima, S. and T. Ichihashi, 1993. Single-shell carbon nanotubes of 1-nm diameter. *Nature*, 363: 603-605.
- Jang, Y.T., S.I. Moon, J.H. Ahn, Y.H. Lee and B.K. Ju, 2004. A simple approach in fabricating chemical sensor using laterally grown multi-walled carbon nanotubes. *Sens. Actuators B*, 99: 118.
- Kang, H.S., 2006. Theoretical study of boron nitride nanotubes with defects in nitrogen-rich synthesis. *J. Phys. Chem. B*, 110(10): 4621.
- Kong, J., N.R. Franklin, C. Zhou, M.G. Chapline, S. Peng, K. Cho and H. Dai, 2000. Nanotube molecular wire as chemical sensors. *Sci.*, 287: 622.
- Liu, Y. and H. Guo, 2004. Current distributions in B- and N-doped carbon nanotubes. *Phys. Rev. B*, 69: 115401.
- Liu, L.V., W.Q. Tian and Y.A. Wang, 2006. Ozonization at the vacancy defect site of the single-walled carbon nanotube. *J. Phys. Chem. B*, 110: 13037.
- Liu, H.J., J.P. Zhai, C.T. Chan and Z.K. Tang, 2007. Density functional theory study of atomic oxygen, O<sub>2</sub> and O<sub>3</sub> adsorptions on the H-capped (5, 0) single-walled carbon nanotube. *Nanotechnology*, 18: 65704.
- Lu, X., Z.F. Chen and P.V. Schleyer, 2005. Are the stone-Wales defects always more reactive than perfect sites in the sidewalls of single-wall carbon nanotubes. *J. Am. Chem. Soc.*, 127: 20.
- Lucken, E.A.C., 1969. Nuclear Quadrupole Coupling Constants. Academic Press, London, ISBN-13: 978-0124584501.
- Mintmire, J.W., B.I. Dunlap, C.T. White, 1992. Are fullerene tubules metallic? *Phys. Rev. Let.*, 68: 631.
- Marian, C.M. and M. Gastreich, 2001. Structure-property relationships in boron nitrides: The <sup>15</sup>N- and <sup>11</sup>B chemical shifts. *Solid State Nucl. Mag.*, 19: 29.
- Mirzaei, M. and N.L. Hadipour, 2006. An investigation of hydrogen-bonding effects on the nitrogen and hydrogen electric field gradient and chemical shielding tensors in the 9-methyladenine real crystalline structure: A density functional theory study. *J. Phys. Chem. A*, 110(14): 4833.
- Mirzaei, M. and N.L. Hadipour, 2007. Study of hydrogen bonds in 1-methyluracil by DFT calculations of oxygen, nitrogen, and hydrogen quadrupole coupling constants and isotropic chemical shifts. *Chem. Phys. Let.*, 438(4-6): 304.
- Miyamoto, Y., 1996. Mechanically stretched carbon nanotubes: Induction of chiral current. *Phys. Rev. B*, 54(14): R11149.
- Parr, R.G. and W. Yang, 1994. Density Functional Theory of Atoms and Molecules. Oxford University Press, ISBN13: 9780195092769.
- Peng, S. and K.J. Cho, 2000. Chemical control of nanotube electronics. *Nanotechnology*, 11: 57.
- Peng, S. and K. Cho, 2003. Ab initio study of doped carbon Nanotube sensors. *Nano Let.*, 3(4): 513-517.
- Perdew, P., K. Burke and Y. Wang, 1996. Generalized gradient approximation for the exchange-correlation hole of a many-electron system. *Phys. Rev. B*, 54: 16533-16539.
- Rubio, A., J.L. Corkill and M.L. Cohen, 1994. Theory of graphitic boron nitride nanotubes. *Phys. Rev. B*, 49(7): 5081.
- Souza Filho, A.G., M. Endo, H. Muramatsu, T. Hayashi, Y.A. Kim, E.B. Barros, N. Akuzawa, G.G. Samsonidze, R. Saito and M.S. Dresselhaus, 2006. Resonance Raman scattering studies in Br<sub>2</sub>-adsorbed double-wall carbon nanotubes. *Phys. Rev. B*, 73: 235413.
- Souza Filho, A.G., V. Meunier, M. Terrones, B.G. Sumpter, E.B. Barros, F. Villalpando-Paez, J.M. Filho, Y.A. Kim, H. Muramatsu, T. Hayashi, M. Endo and M.S. Dresselhaus, 2007. Selective tuning of the electronic properties of co-axial nanocables through exohedral doping. *Nano Let.*, 7: 2383.
- Valentini, L., C. Cantalini, I. Armentano, J.M. Kenny, L. Lozzi and S. Santucci, 2004. Highly sensitive and selective sensors based on carbon nanotubes thin films for molecular detection. *Diamond Relat. Mater.*, 13: 1301.
- Wang, S.G., Q. Zhang, D.J. Yang, P.J. Sellin and G.F. Zhong, 2004. Multi-walled carbon nanotube-based gas sensors for NH<sub>3</sub> detection. *Diamond Relat. Mater.*, 13: 327.
- Wolinski, K., J.F. Hilton and P. Pulay, 1990. Efficient implementation of the gauge-independent atomic orbital method for NMR chemical shift calculations. *J. Am. Chem. Soc.*, 112(23): 8251.
- Wu, G., S. Dong, R. Ida and N. Reen, 2002. A solid-state <sup>17</sup>O nuclear magnetic resonance study of nucleic acid bases. *J. Am. Chem. Soc.*, 124: 1768.
- Zhao, J., A. Martinez-Limia and P.B. Balbuena, 2005. Understanding catalysed growth of single-wall carbon nanotubes. *Nanotechnology*, 16: 575.
- Zurek, E., C.J. Pickard and B.J. Autschbach, 2008. Determining the diameter of functionalized single-Walled carbon Nanotubes with <sup>13</sup>C NMR: A theoretical study. *J. Phys. Chem., C*, 112: 9267.